Nd-doped phosphate glass cane laser: From materials fabrication to power scaling tests

Nd-doped phosphate glass cane laser: from materials fabrication to power scaling tests

Edoardo Ceci-Ginistrelli [1,2], Callum Smith [2], Diego Pugliese [1], Joris Lousteau [2], Nadia G. Boetti [3], W. Andrew Clarkson [2], Francesco Poletti [2], Daniel Milanese [1,4]

[1] Politecnico di Torino, Dipartimento di Scienza Applicata e Tecnologia and INSTM, Corso Duca degli Abruzzi 24, 10129 Torino, Italy

[2] Optoelectronics Research Centre, University of Southampton, SO17 1BJ Southampton, United Kingdom

[3] Istituto Superiore Mario Boella, Via P. C. Boggio 61, 10138 Torino, Italy

[4] Consiglio Nazionale delle Ricerche, Istituto di Fotonica e Nanotecnologie, Via alla Cascata 56/C, 38123 Trento, Italy

* Corresponding author: edoardo.ceciginistrelli@polito.it, Tel: +39 011 0904707, Fax: +39 011 0904699.

Abstract

We report on the fabrication and characterization of two Nd-doped active glasses and two compatible cladding compositions. The materials were synthesized to be compatible in terms of thermal expansion and characteristic temperatures. The glass system with higher refractive index and absorption cross-section was selected for the fabrication of a core/cladding cane with a diameter of 800 µm. Laser experiments, performed on a 60 mm-long cane, show laser emission at 1054 nm with output power higher than 2 W and efficiency above 40%. These values, obtained on a very simple geometry, are promising for the development of short-length cane lasers and amplifiers for emission in the 1 µm region.

Keywords: Phosphate glass; high-power laser; Nd laser; cane laser; laser rod.

1. Introduction

Nd^{3+} ion is a well-known emitter in laser technology. Due to its electronic structure, which is particularly suitable for 4-level laser emission around 1 µm, neodymium has been used in the fabrication of the first fiber laser in 1961 [1] and since then it has been embedded in several host materials, both crystalline and amorphous [2-5].

Noticeable attention was devoted in the past two decades to the study of Nd-doped phosphate glasses. These materials are particularly well suited for compact high-power laser devices as they offer a solubility of rare-earth (RE) ions comparable to that exhibited by crystalline YAG and one order of magnitude higher than that of silica glass [6,7]. Moreover, they show low photo-darkening, low non-linear effects and a mature and large-scale manufacturing technology [8-10]. All these features make them an interesting alternative to traditional silica glasses. Nd-doped phosphate glasses were developed originally for the amplification and generation of high-power laser beams in continuous and pulsed

regimes. The main boost towards the manufacturing of highly efficient RE-doped phosphate glasses occurred for the development of extreme high-power lasers for the study of nuclear fusion, as the one developed at the National Ignition Facility at the LLNL laboratories in the USA [11]. Notwithstanding over 50 years of laser glass development and the availability of commercial products, there is still research interest in the fabrication of new materials with enhanced power scaling possibilities, low cost and easy processing [12,13]. Nowadays, the research is motivated by recent advances in laser-based technologies for several application fields, such as additive manufacturing, surgery or defense. These techniques require the manufacture of reliable, short and compact fiber or cane based lasers with multi-watt or kilowatt output power, low cost and high beam quality.

RE-doped phosphate glasses have been used for the fabrication of fiber lasers and amplifiers and are widely employed [7,14,15]. However, they have shown problems arising from the limited integration with silica based passive optical components. The difference in refractive index between the silica and the phosphate networks can result in significant insertion loss and the presence of hot points. Moreover, power loss is also due to defects at the core/cladding interface which can occur during the fabrication process. A possible solution to these issues relies in the design and fabrication of large core fibers or canes to be used for laser generation and amplification. These structures can be utilized as high power lasers, benefiting from an increased threshold for the onset of non-linear effects and a simple heat-sinking configuration [16]. The biggest limiting factor to the further development of such devices is the high thermal loading experienced by phosphate glasses due to their lower thermal conductivity compared to YAG [2], inducing severe mechanical stress to the device [17-19]. Thermal dilatation occurring in consequence of overheating causes misalignment of the optical set-up, beam distortion and fracture at the core/cladding interface of the fiber. The thermal compatibility between the core and the cladding of a device becomes even more critical when aiming to fabricate a cane laser. In these conditions, there is an increase of the interface stress both during the cane drawing process and the laser testing. Low thermal expansion and optimal thermo-mechanical compatibility between the core and cladding materials of optical fibers become thus mandatory in order to develop highly efficient devices. Often, the scarce compatibility between commercially available active materials and passive cladding compositions leads to poor device efficiency, in consequence of the insurgence of mechanical stress [12]. An attempt to overcome such limitations was proposed by Fujimoto and Nakatsuka [20,21] using silica glass. The strategy developed allows doping SiO_2 with amounts of Nd_2O_3 up to 3 wt%; however, this method does not seem to be scalable to industrial production in terms of quality and quantity [22]. Indeed, previous experience seems to lead to the evidence that the technological limit reached by the development of efficient short-length high-power lasers could be overcome by the design of more efficient materials with enhanced properties and excellent thermo-mechanical compatibility [23].

In this work, two pairs of phosphate glass compositions (two cores and two claddings) were carefully designed to meet the requirements of a cane laser in a core/cladding configuration. The materials were then fabricated and fully characterized. Particular attention was devoted to maintain an optimal matching of thermal expansion coefficients, increase stability against crystallization and provide sufficient refractive index mismatch for effective light guiding. One active and one passive glass with a difference in the coefficient of thermal expansion of 0.2×10^{-6} K^{-1} and a difference in the glass transition temperature below 10 °C were selected. High glass transition temperature and relatively low values of thermal expansion coefficient were also seeked in order to guarantee sufficient robustness to the bulk materials. The glasses were drawn into an 800 µm cane to be used for the demonstration of the first example, to the best of our knowledge, of a phosphate glass cane laser in a core/cladding configuration. The preliminary results on laser emission upon 795 nm pump excitation proved a good power scaling ability, showing a slope efficiency of 44% with respect to absorbed pump power and a maximum emitted power of 2.5 W. These values are comparable with those obtained so far on similar devices [19]. No signs of damage could be observed on the devices in consequence of thermal overload. The Caird analysis [24] performed on the cane confirms that further increase of the efficiency may be obtained by improving the heat sinking and limiting the loss of the system. The estimated intrinsic slope efficiency value matches those obtained so far on phosphate and silicate photonic crystal fibers [12,25]. By walking the full path from the raw materials to the power scaling tests of a cane laser, we demonstrated that a careful design of the material composition can effectively improve the efficiency of the material, facilitate the cane fabrication process and lower the overall fabrication costs, thus encouraging further research in this field.

2. Materials and methods

2.1 Glass fabrication and characterization

Two phosphate glass hosts (CL1: P_2O_5, K_2O, Al_2O_3, B_2O_3, SiO_2, PbO and CL2: P_2O_5, K_2O, Al_2O_3, B_2O_3, SiO_2, Nb_2O_5) were *ad hoc* developed for this research in order to be robust, highly stable against crystallization and suitable for cane drawing.

Based on these compositions, two core and two cladding glasses named respectively CL1:Nd (Nd^{3+} ions concentration $7.2 \times 10^{+19}$ cm^{-3}), CL2:Nd (Nd^{3+} ions concentration $7.5 \times 10^{+19}$ cm^{-3}), CL1 and CL2, were synthesized by conventional melt-quenching technique and thoroughly characterized. These glasses were designed to guarantee a suitable refractive index contrast and at the same time an enhanced thermo-mechanical compatibility. In view of fulfilling both these requirements, the core and cladding glasses were fabricated by doping the glass hosts with 4.7 mol% La_2O_3 and 0.3 mol% Nd_2O_3 and with 2 mol%

La_2O_3 and 3 mol% SiO_2, respectively, with the total amount of the components being 100 mol% for all the glasses manufactured.

High purity chemicals (99+%) were mixed in a glove box according to the planned compositions in order to minimize the water content in the glasses. The batched chemicals were melted at a temperature of 1400 °C for 1 h in a vertical furnace under a controlled atmosphere (dry air, water content < 3 ppm) and subsequently cast in a preheated brass mold. The cast glasses were immediately annealed at a temperature around the transition temperature, T_g, for 12 h to relieve internal stresses and finally cooled down slowly to room temperature. The core glass compositions (CL1:Nd and CL2:Nd) were cast in a cylindrical mold with a diameter of 12 mm to obtain 10 cm-long rod preforms. The cladding glass compositions (CL1 and CL2) were shaped in the form of a tube by rotational casting [27] at a rotation speed of 3000 rpm using a dedicated equipment designed and built *in-house*. The external surface of the core rods and of the cladding tubes was polished carefully with SiC papers of different grits and 1 μm diamond paste.

Flat specimens were cut from all the preforms and optically polished to 1 mm-thick samples to be used for optical and spectroscopic characterizations.

The density of the glasses was measured at room temperature by the Archimedes' method by using distilled water as immersion fluid. The Nd^{3+} ions concentrations were calculated through density data in relation to the nominal composition of the glasses.

The characteristic temperatures of the glasses (glass transition temperature T_g and onset crystallization temperature T_x) were measured using a Netzsch DTA 404 PC Eos differential thermal analyzer with a heating rate of 5 °C/min in sealed Pt/Rh pans. The coefficient of thermal expansion (CTE) was measured by a horizontal alumina dilatometer (Netzsch, DIL 402 PC) operating at 5 °C/min on 5 mm-long specimens. The measure was automatically interrupted when a shrinkage higher than 0.13% was reached (softening point). CTE values were calculated in the 200-400 °C temperature range.

The refractive index of the glasses was measured at 633 and 1061 nm by prism coupling technique (Metricon, model 2010). The estimated error of the measurement was ± 0.001.

The absorption spectra were measured on the core samples to identify the Nd^{3+} characteristic peaks. The measurement was performed at room temperature for wavelengths ranging from 300 to 900 nm using a double beam scanning spectrophotometer (Varian Cary 500).

Continuous-wave (CW) photoluminescence spectra in the near-infrared region were acquired by a Jobin Yvon iHR320 spectrometer equipped with a Hamamatsu P4631-02 detector, using standard lock-in technique. Emission spectra were obtained by exciting the sample with a monochromatic light at 785 nm, emitted by a fiber pigtailed laser diode (Axcel B1-785-1400-15A).

The fluorescence lifetime of Nd^{3+}:$^4F_{3/2}$ level was obtained by exciting the samples with light pulses of the 785 nm laser diode, recording the signal by a digital oscilloscope (Tektronix TDS350) and fitting

the decay traces by a single exponential. Estimated error of the measurement was ± 20 μs. The detector used for this measurement was a Thorlabs PDA10CS.

All measurements were performed at room temperature.

2.2 Cane fabrication and characterization

The canes used for preliminary laser tests were manufactured using the CL1:Nd and the CL1 compositions, as they proved to be more suitable for this application (see Sections 3.2 and 3.3). The final preform was fabricated by the rod-in-tube method and stretched by cane drawing. The core rod was obtained by stretching the 12 mm diameter preform obtained by melt-quenching into a thinner cylinder with a diameter of 3 mm. The cladding tube was manufactured by rotational casting, as explained in Section 2.1. Both the core stretching and the cane drawing were made using an *in-house* developed drawing facility. The obtained canes presented a diameter of 800 μm and a core/cladding diameter ratio of 1/3.

2.3 Laser tests

An experiment (Fig. 1) was conducted to investigate the performance of the canes (see Section 2.2) in a laser configuration. A 60 mm length of cane, with a core diameter of 270 μm and a cladding diameter of 800 μm, was used as the active gain medium. The cane was submerged in a water bath, which provided essential heat-sinking and acted as a guiding interface for the pump radiation. The end-faces of the cane were optically polished. The cane was pumped by a fiber-coupled diode laser operating at 795 nm, with a core diameter of 200 μm and a Numerical Aperture (NA) of 0.22. The output of the pump delivery fiber was imaged into the cane using two lenses acting as a 1:2 imaging system, thus creating a 400 μm diameter pump spot with a NA of 0.11 at the front face of the cane, which satisfies the conditions for guiding in the cladding. A laser cavity was implemented by aligning appropriate mirrors close to the faces of the cane. At the pump input face a mirror with high transmission at 795 nm and high reflection at 1054 nm was positioned, whilst at the other end an output coupler mirror was placed. The output radiation was collected by a lens and sent to a dichroic mirror angled at 45° with high reflection at 1054 nm and high transmission at 795 nm. Therefore, residual pump radiation can be split from the laser signal. The remaining pump power was sent to a beam dump, whilst the laser signal power was sent on to diagnostics.

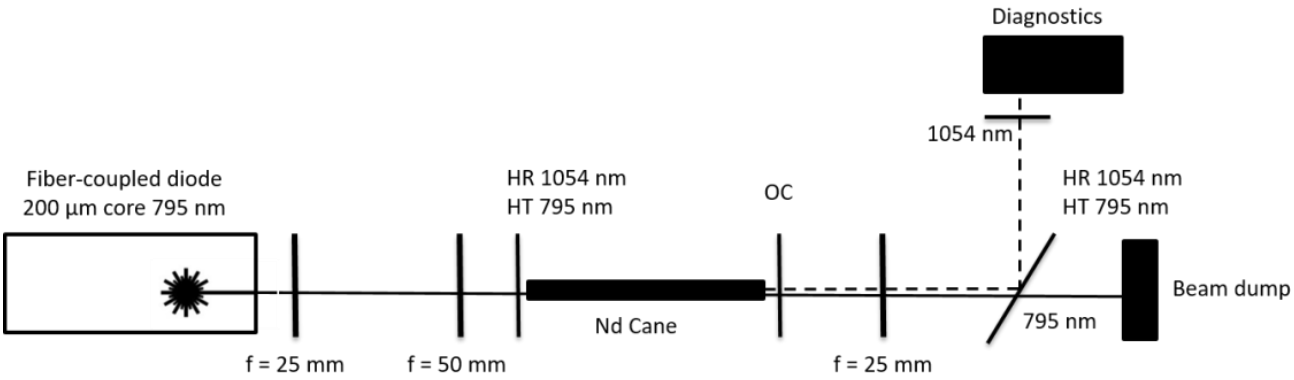

Fig. 1. Setup used for the laser experiments.

3. Results and discussion

3.1. Glass physical and thermal properties

The fabrication of large diameter fibers, also known as cane lasers, has proven to be challenging due to some technological limits arising from the processing of their constituent materials. In particular, failure of the drawing procedure can occur due to fracturing of the glasses in the drawing facility in consequence of a thermal shock. The glass compositions developed for this research have overcome this issue and proved to be robust and resistant to the thermal stress induced by their processing. Table 1 reports the thermal, physical and fluorescence properties of the glasses compared to some existing commercial materials. Thermal analysis reveals a stability parameter ΔT above 250 °C for all the manufactured materials, proving that they are stable against crystallization and suitable for cane drawing. The CTE measurements show values of thermal expansion lower than those exhibited by the most common glasses available [12,28] and comparable to those reported for QX/Nd glass fabricated by Kigre [29]. Furthermore, it is worthwhile noting the minimal difference in terms of thermal expansion between the fabricated core and cladding glasses. This matching is fundamental when operating the laser in a high-power regime, as it limits the tensile stress at the core/cladding interface of the cane due to thermal expansion.

Table 1

Glass transition temperature (T_g), crystallization temperature (T_x), stability parameter (ΔT), density, coefficient of thermal expansion and Nd^{3+}:$^4F_{3/2}$ fluorescence lifetime of the manufactured phosphate glasses and of the commercially available LG-770 (Schott) and QX/Nd (Kigre) glasses.

Glass label	T_g [°C] ± 3 °C	T_x [°C] ± 3 °C	$\Delta T = T_x - T_g$ [°C] ± 6 °C	ρ [g/cm^3] ± 0.05 g/cm^3	CTE [10^{-6} K^{-1}] ± 0.1 K^{-1}	Nd^{3+}:$^4F_{3/2}$ fluorescence lifetime [µs] ± 20 µs
CL1:Nd	522	790	268	3.01	8.1	326
CL2:Nd	593	958	365	2.80	7.1	350
CL1	530	808	278	2.91	8.3	n.a.
CL2	610	>1000	>390	2.67	7.4	n.a.
LG-770 [23]	461	n.a.	n.a.	2.56	13.4	350
QX/Nd [24]	506	n.a.	n.a.	2.66	8.4	353

3.2. Refractive index

Table 2 reports the refractive indices of the fabricated core and cladding glasses and of the commercial LG-770 and QX/Nd glasses measured at the wavelengths of 633 and 1061 nm. The refractive indices of the manufactured glasses are higher than the ones reported for commercial compositions. This is generally desirable for high-power laser applications, as it facilitates fabricating thermally compatible low refractive index cladding glasses for the manufacturing of double-cladding optical fibers [30,31]. The CL1:Nd glass showed the highest value of refractive index at the laser wavelength, thus resulting in the optimal core composition for the fabrication of the canes. The coupling of the CL1:Nd core glass to the relative cladding CL1 leads to a NA value of 0.16, which allows a good confinement of the laser radiation into the core of the cane.

Table 2

Refractive indices of the manufactured glasses in comparison with those of commercial compositions.

Glass label	n @ 633 nm	n @ 1061 nm
CL1:Nd	1.557	1.548
CL2:Nd	1.551	1.540
CL1	1.549	1.540
CL2	1.543	1.533
LG-770 [22]	1.507	1.450
QX/Nd [14]	1.536 (n_c)	1.530

3.3. Absorption spectroscopy

High values of absorption cross-section at the excitation wavelength are desirable in order to increase the efficiency of the material in absorbing the pump light. Fig. 2b depicts the UV-Visible (UV-Vis) spectra of

the two core compositions (CL1:Nd and CL2:Nd) in the 300 to 900 nm wavelength region. The observed peaks can be directly correlated to the corresponding energy levels shown in Fig. 2a. The absorption cross-section was calculated according to the following equation:

$$\sigma_a = \frac{2.303 \log\left(\frac{I_0}{I}\right)}{NL}$$

where $log(I_0/I)$ is the glass absorbance, L is the sample thickness expressed in cm and N is the Nd^{3+} ions concentration per cm^3. The values of the cross-section measured at the typical excitation wavelength of 800 nm are $\sigma_a = 2.3 \times 10^{-20}$ cm^{-1} for the CL1:Nd glass and $\sigma_a = 2.0 \times 10^{-20}$ cm^{-1} for the CL2:Nd glass. This suggests that the CL1:Nd glass offers a more favorable environment with respect to the CL2:Nd for the exploitation of the $^4F_{3/2} \rightarrow {}^4I_{11/2}$ transition. Generally, both these values are comparable to those reported in literature for commercial compositions [28,29]. Moreover, it is worthwhile noting that an opposite trend can be observed for the main absorption peak located at 580 nm; in this region, the CL2:Nd glass shows higher values of absorption cross-section, thus suggesting that the excitation of the $^4G_{5/2}$ level is favored for this glass.

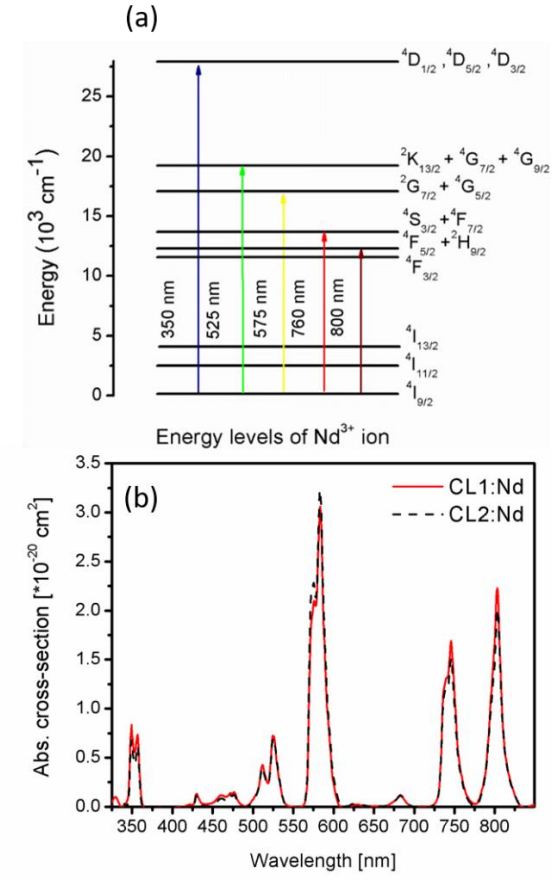

Fig. 2. (a) Energy levels of Nd^{3+} ion; (b) absorption spectra of the CL1:Nd and CL2:Nd glasses.

3.4. Infrared luminescence spectroscopy and time-resolved fluorescence spectroscopy

Fig. 3 depicts the normalized emission spectra of CL1:Nd and CL2:Nd glasses in the region between 1010 and 1130 nm recorded upon excitation at the wavelength of 785 nm. The peak centred at 1054 nm is correlated to the Nd^{3+}:$^4F_{3/2} \rightarrow {}^4I_{11/2}$ transition in phosphate glass and is exploited for laser emission. No variation in the shape of the peak can be noticed for the two glasses.

The lifetimes of the $^4F_{3/2}$ excited state, upon 785 nm excitation, were measured by time-resolved fluorescence spectroscopy, and the results are reported in the last column of Table 1. The values measured are 326 µs for the CL1:Nd glass and 350 µs for the CL2:Nd glass and match with our previous measurements on similar glasses and with those reported in literature for commercial compositions [10, 28,29,32]. A higher lifetime value is favorable for lasing action as it benefits population inversion, thus making the CL2:Nd glass more suitable for laser action. However, this material also shows lower absorption cross-section at the excitation wavelength (see Fig. 2b) resulting in a lower efficiency of pump absorption.

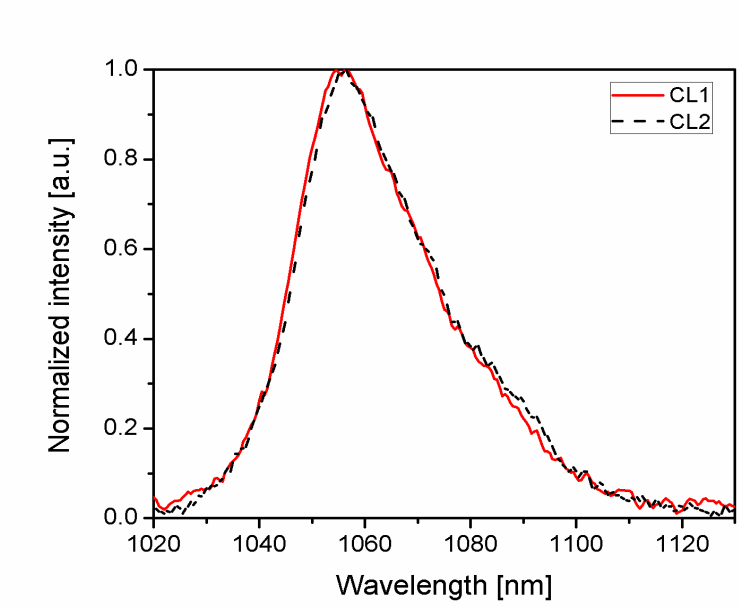

Fig. 3. Normalized emission spectra of CL1:Nd and CL2:Nd glasses centred at 1054 nm.

3.5. Cane characterization

The results concerning the characterization of the bulk materials, presented in the former sections, suggest that the combination of CL1:Nd and CL1 glasses is the most promising for an effective laser application. Despite the fact that CL2:Nd exhibits a higher time-resolved fluorescence lifetime and lower thermal expansion coefficient, the CL1 compositions show good thermo-mechanical properties, higher refractive

index and higher absorption cross-section at the excitation wavelength, combined with lower viscosity and thus easier processing. For such reasons, these materials were chosen for the fabrication of core/cladding canes following the procedure explained in Section 2.2. Such canes have been used in laser testing. Fig. 4 portraits the typical cross-section of the 800 µm-diameter cane. No significant defects in size, shape or in the core/cladding interface could be observed at the optical microscope, proving the good control on the fabrication process.

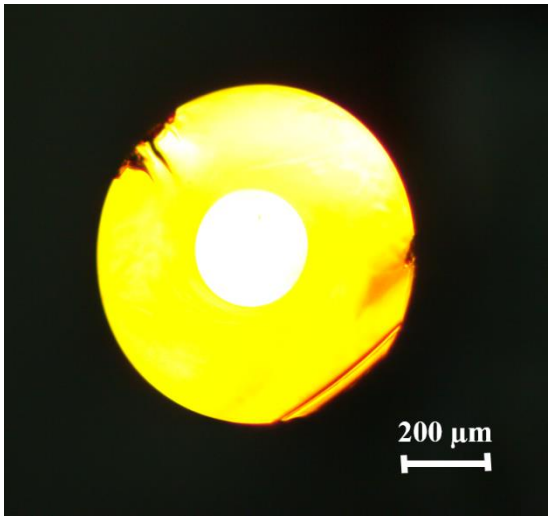

Fig. 4. Typical cross-section of the fabricated core/cladding cane.

3.6. Laser tests

Several output couplers ranging from 50-95% reflectivity at 1064 nm were used in the setup (see Fig. 5), with the highest output power being achieved for a 70% reflectivity output coupler. Laser operation occurred on numerous longitudinal modes at around 1054 nm, which is consistent with the fluorescence spectrum (see Section 3.4). The cane supported a very large number of transverse modes, and therefore the output beam was highly multimodal. Fig. 5 shows the lasing spectrum and beam profile at the maximum output power of 2.5 W.

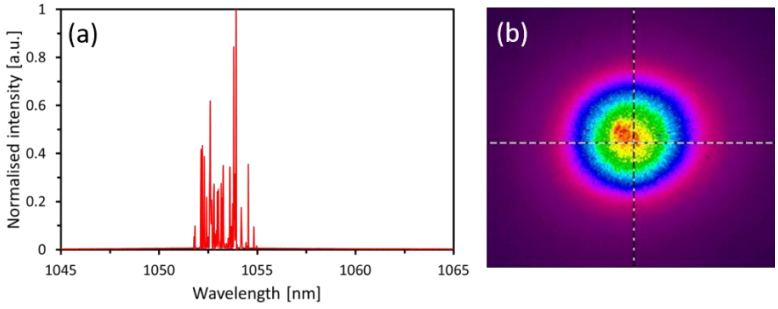

Fig. 5. Lasing wavelength (a) and beam profile (b) at the maximum output power.

The laser output power was recorded as a function of the launched and absorbed pump powers (see Fig. 6). The loss of the pump radiation due to the scattering within the bulk cane material and at the core/cladding and cladding/water interfaces was approximated by investigating the losses at 975 nm. Neodymium exhibits negligible absorption at 975 nm, therefore by launching this wavelength in a similar manner to that described for the 795 nm fiber-coupled diode laser (see Section 2.3), one can estimate the pump guiding loss, which was approximately 10 dB/m. The absorbed pump power was estimated by first considering the lost pump power, i.e. the launched pump power minus the remaining unabsorbed pump power, and then incorporating the pump guiding loss term estimated from the 975 nm transmission. The absorbed pump power was approximately 65% of the launched pump power. A maximum output power of 2.5 W was achieved for a launched/absorbed pump power of 19.0 W/12.5 W. This corresponds to a slope efficiency of 30% with respect to the launched pump power and 44% with respect to the absorbed pump power.

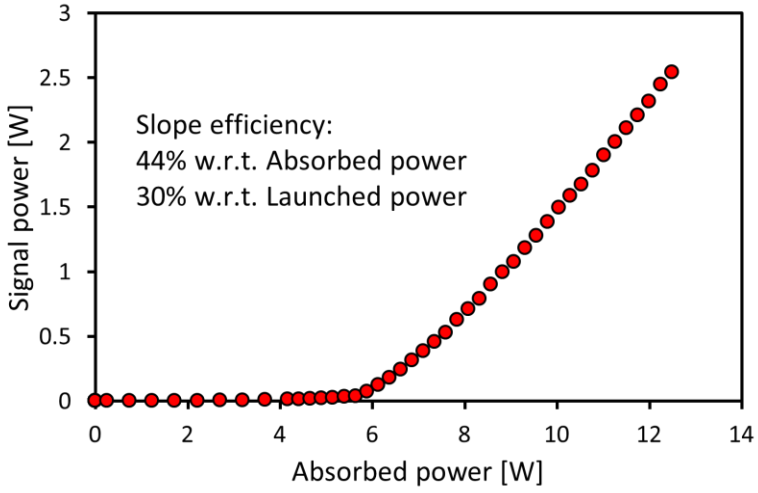

Fig. 6. Output power as a function of the absorbed pump power.

It was found that the best performance was achieved when the cavity mirrors were slightly offset from the cane end-faces by approximately 500 μm. This slight separation is necessary as when the cane heats up due to pump power absorption, it expands. This expansion can cause the cane to push against the mirrors and result in misalignment. The distance between the end-faces and the mirrors allows the cane to expand without contacting the mirrors and thus prevents this deleterious misalignment.

The cane losses for the signal radiation were estimated using the Findlay-Clay analysis [33]. This technique involves measuring the threshold lasing power, P_{th}, at the signal wavelength for a variety of output couplers with different reflectivity, R. Plotting $-ln\ R$ against P_{th} should yield a straight line, with

the intercept of this line representing the round-trip loss for the laser. Fig. 7a shows this plot, leading to a loss of 4.6 dB/m. A second estimation of the loss is achievable by plotting the reciprocal of the slope efficiency as a function of the reciprocal of the output couplers transmission. This method is known as Caird analysis [24] and also provides an estimate of the maximum efficiency obtainable from the active material of the laser. Fig. 7b depicts the results of the Caird analysis, which brought about a loss of 6.1 dB/m and an intrinsic slope efficiency of 55%. The two methods led to comparable loss values, slightly higher than those obtained on other phosphate glass fibers [8,15,18]. Further reduction of the loss may be attained during manufacturing by improving the glass homogeneity.

The estimated intrinsic slope efficiency matches the maximum efficiency values achieved on multi-core photonic-crystal fibers [14], although it is still lower if compared to photonic-crystal silicate fibers [25].

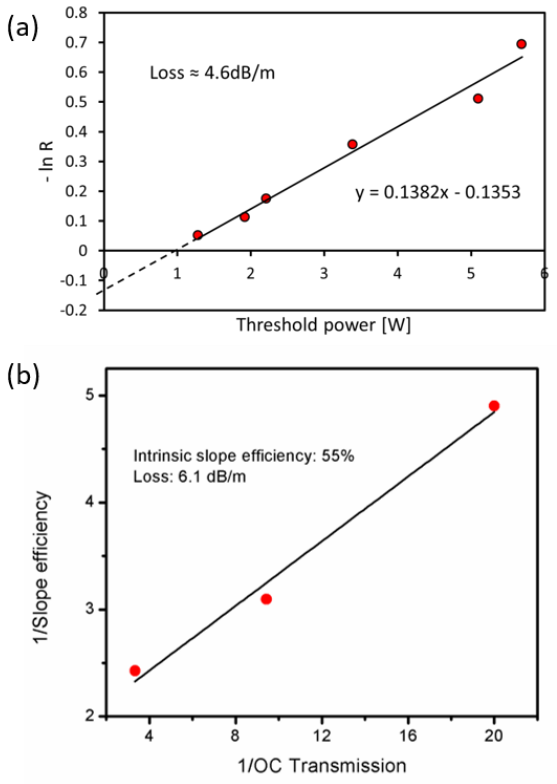

Fig. 7. Resonator losses estimated from the threshold pump power (Findlay-Clay analysis) (a) and from the slope efficiency (Caird analysis) (b) for various output couplers.

4. Conclusion

In this work we designed, manufactured and fully characterized two core and two cladding compositions able to satisfy the thermo-mechanical compatibility conditions imposed by the small size and high-power density of cane lasers and amplifiers.

The synthesized materials combine good efficiency and optical properties with low thermal expansion, excellent resistance against crystallization and suitability for cane drawing. The glasses were processed through rotational casting and cane drawing without showing any sign of damage or degradation. It was demonstrated that a careful matching of the properties of the core and cladding glasses is able to overcome the difficulties in the cane drawing and minimize the interface stress. This results in a higher slope efficiency of the laser.

A laser device was successfully fabricated and tested in CW mode registering a slope efficiency of 44% with respect to the absorbed pump power and an output power of 2.5 W. The Caird analysis resulted in an intrinsic slope efficiency of 55%, thus encouraging further work in order to improve its current value.

Further research is encouraged towards the enhancement of the laser performance by improving the glass homogeneity and reducing the loss of the system. Moreover, the pump absorption efficiency can be increased by manufacturing double-cladding canes with asymmetrical structures.

Acknowledgments

The authors acknowledge the COST Action MP1401 “Advanced Fibre Laser and Coherent Source as Tools for Society, Manufacturing and Lifescience” for the partial support of this research effort.

References

[1] E. Snitzer, Phys. Rev. Lett. 7 (1961) 444–446.

[2] M. Yamane, Y. Asahara, Glasses for Photonics, Cambridge University Press, Cambridge, 2000.

[3] A. Agnesi, L. Carrà, G. Reali, Opt. Mater. 30 (2008) 1828–1831.

[4] S. Sattayaporn, G. Aka, P. Loiseau, A. Ikesue, Y.L. Aung, J. Alloys Compd. 711 (2017) 446–454.

[5] S. Kang, X. Wang, W. Xu, X. Wang, D. He, L. Hu, Opt. Mater. 66 (2017) 287–292.

[6] J.H. Campbell, T.I. Suratwala, J. Non-Cryst. Solids 263-264 (2000) 318–341.

[7] A.L.F. Novais, N.O. Dantas, I. Guedes, M.V.D. Vermelho, J. Alloys Compd. 648 (2015) 338–345.

[8] N.G. Boetti, G.C. Scarpignato, J. Lousteau, D. Pugliese, L. Bastard, J.-E. Broquin, D. Milanese, J. Opt. 17 (2015) 065705.

[9] D. Pugliese, N. G. Boetti, J. Lousteau, E. Ceci-Ginistrelli, E. Bertone, F. Geobaldo, D. Milanese, J. Alloys Compd. 657 (2016) 678–683.

[10] L. Hu, D. He, H. Chen, X. Wang, T. Meng, L. Wen, J. Hu, Y. Xu, S. Li, Y. Chen, W. Chen, S. Chen, J. Tang, B. Wang, Opt. Mater. 63 (2017) 213–220.

[11] J.H. Campbell, J.S. Hayden, A. Marker, Int. J. Appl. Glass Sci. 2 (2011) 3–29.

[12] Q. Yin, S. Kang, X. Wang, S. Li, D. He, L. Hu, Opt. Mater. 66 (2017) 23–28.

[13] Y.B. Saddeek, A.A. El-Maaref, K.A. Aly, M.M. Elokr, A.A. Showahy, J. Alloys Compd. 694 (2017) 325–332.

[14] L. Wang, D. He, S. Feng, C. Yu, L. Hu, D. Chen, Laser Phys. 26 (2016) 015104.

[15] Y.W. Lee, S. Sinha, M.J.F. Digonnet, R.L. Byer, S. Jiang, Opt. Lett. 31 (2006) 3255–3257.

[16] X. Délen, Y. Zaouter, I. Martial, N. Aubry, J. Didierjean, C. Hönninger, E. Mottay, F. Balembois, P. Georges, Opt. Lett. 38 (2013) 109–111.

[17] J.H. Campbell, Recent advances in phosphate laser glasses for high power applications, in: P. Klocek (Ed.), Inorganic Optical Materials, SPIE, Washington, 1996, pp. 3–39.

[18] N.G. Boetti, J. Lousteau, E. Mura, S. Abrate, D. Milanese, ICTON 2014 (2014) 6876634.

[19] R.A. Martin, J.C. Knight, IEEE Photon. Technol. Lett. 18 (2006) 574–576.

[20] Y. Fujimoto, M. Nakatsuka, J. Non-Cryst. Solids 215 (1997) 182–191.

[21] M. Murakami, M. Yoshida, H. Nakano, Y. Fujimoto , H. Shiraga, S. Motokoshi, S. Matsuoka, J. Maeda, H. Kan, J. Non-Cryst. Solids 357 (2011) 963–965.

[22] M. Tiegel, A. Herrmann, C. Rüssell, J. Körner, D. Klöpfel, J. Hein, M.C. Kaluza, J. Mater. Chem. C 1 (2013) 5031–5039.

[23] J. Ballato, P. Dragic, J. Am. Ceram. Soc. 96 (2013) 2675–2692.

[24] J.A. Caird, S.A. Payne, P.R. Staber, A.J. Ramponi, L.L. Chase, W.F. Krupke, IEEE J. Quantum Electron. 24 (1988) 1077–1099.

[25] L. Wang, W. Li, Q. Sheng, Q. Zhou, L. Zhang, L. Hu, J. Qiu, D. Chen, J. Lightwave Technol. 32 (2014) 1116–1119.

[26] L. Wang, H. Liu, D. He, C. Yu, L. Hu, J. Qiu, D. Chen, Appl. Phys. Lett. 104 (2014) 131111.

[27] E. Mura, J. Lousteau, D. Milanese, S. Abrate, V.M. Sglavo, J. Non-Cryst. Solids 362 (2013) 147–151.

[28] www.schott.com

[29] www.kigre.com

[30] M.J.E. Digonnet, Rare-Earth-Doped Fiber Lasers and Amplifiers, CRC Press, Boca Raton, 2001.

[31] D. Dorosz, Bull. Pol. Acad. Sci., Tech. Sci. 56 (2008) 103–111.

[32] N.G. Boetti, D. Negro, J. Lousteau, F.S. Freyria, B. Bonelli, S. Abrate, D. Milanese, J. Non-Cryst. Solids 377 (2013) 100–104.

[33] D. Findlay, R.A. Clay, Phys. Lett. 20 (1966) 277–278.